1994

Interstellar gas and dust in the young cluster IC 348

Theodore P. Snow

Margaret Murray Hanson

C Gregory Seab
University of New Orleans

Jon M. Saken

THE ASTROPHYSICAL JOURNAL, 420:632–642, 1994 January 10

INTERSTELLAR GAS AND DUST IN THE YOUNG CLUSTER IC 348

THEODORE P. SNOW[1,2]
Research Centre for Theoretical Astrophysics, University of Sydney; and Center for Astrophysics and Space Astronomy, University of Colorado
MARGARET MURRAY HANSON
Center for Astrophysics and Space Astronomy, CB 389 University of Colorado, Boulder, CO 80309
C. GREGORY SEAB[1]
Department of Physics, University of New Orleans, Lakefront, New Orleans, LA 70148
AND
JON M. SAKEN
Center for Astrophysics and Space Astronomy, CB 389, University of Colorado, Boulder, CO 80309
Received 1992 November 9; accepted 1993 July 20

ABSTRACT

We have completed a multiband absorption- and emission-line study of a star embedded in the young cluster IC 348, to determine the environmental effect of star formation on the interstellar medium (ISM) local to the region. The hottest and youngest star in IC 348 is BD +31°643, a B5 V star which samples the inner bright nebular region. The nearby star *o* Per, which lies only 8′ to the north and is thought to lie beyond IC 348, samples the gas and dust which has not been processed by very recent star formation. We speculate that the ISM throughout the region was originally the same as that currently seen toward *o* Per, but now the contrasting environmental conditions due to the recent star formation have led to marked differences in the atomic, molecular, and dust characteristics of IC 348. These contrasts include what we have termed a "composite" UV extinction curve for BD +31°643, evidence for enhanced density and enhanced depletions within IC 348 and very different molecular abundances in the interstellar sightline to BD +31°643. Toward BD +31°643, we find a higher column density of CH, but lower CN and very much higher CH^+ than measured toward *o* Per. We conclude that the physical and chemical state of the gas and dust has been altered by local processes and conditions within IC 348.

The characteristics of the ISM in IC 348, via our study of the star BD +31°643, closely resemble those seen toward ρ Oph, another sight line passing through a bright nebular region. However, the stars are not as hot in IC 348 as in Ophiuchus, so their effect on the local ISM is not as severe.

Subject headings: dust, extinction — ISM: abundances — open clusters and associations: individual (IC 348)

1. INTRODUCTION

Comparative studies of interstellar material toward different stars embedded within the same cloud region can be helpful in revealing how various physical and chemical processes progress as functions of cloud density or other environmental factors that may vary within the cloud. The best example of this is the ρ Oph cloud, which contains a number of bright early-type stars at various depths within the cloud. Comparative analysis of these stars has revealed a progression of increasing grain size with depth (Carrasco, Strom, & Strom 1973), for example, and has shown how the depletions change from place to place within the cloud (Snow & Jenkins 1980).

Another dense cloud region of interest, but one which contains no bright stars comparable to those in the ρ Oph cloud, is IC 348, consisting of a small cluster of stars and reflection nebulosity just to the south of *o* Per. This cluster was noted by Gingerich (1922) and has been identified as dynamically bound by studies of proper motions (e.g., Frederick 1956; Duboshin et al. 1976). Attention was drawn to the interstellar matter within the cluster by Strom, Strom, & Carrasco (1974), who found similarities to the ρ Oph cloud in that the dust grains appear to be larger in size in the denser portions of the cloud.

This paper reports on ground-based spectroscopic studies of interstellar lines in the spectrum of the brightest member of the cluster, the star BD +31°643 (aka HDE 281159; the star is classified B5 V and has $V = 8.53$ and $E[B-V] = 0.84$; original photometry are from the compilation of Racine 1968). Data were obtained using the Canada-France-Hawaii Telescope on Mauna Kea using the coudé spectrograph and Reticon detector system to obtain high-dispersion spectra of several lines of interest. The analysis of the data is done largely by comparison with the extensive information available on *o* Per, which lies behind a portion of the same interstellar cloud complex (Sancisi 1974; Sancisi et al. 1974), and whose interstellar absorption lines in both the optical and the ultraviolet have been analyzed in detail (Chaffee 1974; Snow 1975, 1976). From the comparison with *o* Per, as well as *IUE* low-dispersion ultraviolet spectra, it has proved possible to assemble a comprehensive picture of the interstellar gas and dust in IC 348, along the path length to BD +31°643.

The next section summarizes the general properties of the cloud and the line of sight, drawing heavily on literature data on radio emission observations. Following that, § 3 discusses the optical spectroscopy obtained at the Canada-France-Hawaii Telescope; § 4 describes the derivation of the ultraviolet extinction curve from *IUE* spectra; § 5 discusses the far-infrared images of the region, as observed by *IRAS*; § 6 presents discussion and conclusions that can be drawn from all

[1] Guest Observer, Canada-France-Hawaii Telescope.
[2] Postal Address: Center for Astrophysics and Space Astronomy, CB 389, University of Colorado, Boulder, CO 80309.

the disparate forms of data; and § 7 summarizes the principal conclusions and provides comments on future work.

2. GENERAL PROPERTIES OF THE REGION

2.1. *The Cluster and Its Associated Interstellar Material*

Figure 1 (Plates 12 and 13) is a reproduction of the Palomar survey image of the region containing o Per and the loose grouping IC 348. IC 348 was first noted by Gingerich (1922) and has since been included in several studies of gas and dust in the Perseus region (e.g., Blaauw 1952; Borgman & Blaauw 1963). The cluster itself is part of the Perseus II complex (Blaauw 1952; Harris, Morgan, & Roman 1954; Lynds 1969). More recently, Sancisi (1974), Sancisi et al. (1974), Loren (1976), and Sargent (1979) have incorporated radio H I and molecular emission-line data into a comprehensive view of the region. In their picture, star formation has taken place in OB associations where subsequent supernova explosions have created swept-up shells of gas and dust. The bright stars o, ζ, and ξ Per are thought to be moving away from the Earth at the velocity imparted by their formation in one such expanding shell, which has since slowed and now lies between us and these stars. IC 348 is younger and still lies within the expanding shell. This view is supported by the fact that IC 348 contains many young emission-line objects (Herbig 1954), and by the fact that it clearly is embedded within dense material, rather than lying behind it. The brightest star in the cluster, BD +31°643, is a B5 V object and therefore does not excite a large H II region, but studies of both radio CO emission (Kutner et al. 1980) and optical reflection nebulosity (Witt & Schild 1986) show that the star is local to the gas and dust concentration and probably lies within it. (This view had been adopted by Sancisi 1974 and Sancisi et al. 1974, based largely on the obvious coincidence on the sky between the location of the star and the peak of dust extinction and radio emission maps, which themselves show a very close match between the distributions of gas and dust.)

Following the 21 cm work of Sancisi (1974), additional radio observations of the region have been made by others, and now there are radio data available on CH (Sancisi et al. 1974; Zuckerman & Turner 1975; Lang & Willson 1978; Willson 1981); OH (Crutcher 1973; Sancisi et al. 1974), and CO (Kutner et al. 1980; Dickman 1980; Sargent 1979; Bachiller et al. 1987). These observations are very helpful in the present analysis of optical interstellar lines, because they provide velocity and line width information as well as column densities, often covering the positions of both o Per and BD +31°643.

The current expansion velocity of the supernova shell in which IC 348 is embedded is approximately +12–+15 km s^{-1} (heliocentric; or +7–+9 km s^{-1} LSR; all velocities throughout this paper will be heliocentric) and is traced in the velocity of the interstellar medium (ISM) features in front of o Per. The three well-studied bright stars ζ, ξ, and o Per have stellar velocities of +20, +70, and +19 km s^{-1}, respectively, presumably reflecting the higher velocity of the expanding shell at the time when these stars were formed. All three are evolved, and hence are older than IC 348, which consists of main-sequence and pre–main-sequence objects. Thus the velocities of the stars are consistent with the picture painted by Sancisi (1974), in which the stars are now well beyond the expanding shell, which has slowed as it plowed into ambient interstellar gas and dust.

2.2. *The Star*

Optical and near-infrared photometry of several of the brighter members of IC 348 is given by Strom et al. (1974). For BD +31°643, spectral class B5 V, the $B-V$ color is 0.70, which yields $E(B-V) = 0.84$, based on the intrinsic colors of Johnson (1966). The K magnitude is 6.47, and the near-IR colors are $H-K = 0.22$ and $K-L = 0.03$, leading to the color excesses $E(V-K) = 2.53$ and $E(V-L) = 2.57$. Use of the canonical relationship $A_V = 1.1E(V-K)$ yields $A_V = 2.78$ and a value for the ratio of total to selective extinction of $R = 3.31$.

BD +31°643 appears in the Aitkin Double Star catalog as ADS 2730. The star is described as a triple system, with components A and B separated by less than 1″ (the separation varied from 0.″45 to 0.″70 between 1880 and 1924). Component C is farther away, having a separation from A of 23.″5. Thus the photometry of BD +31°643 in the literature must include both the A and B components. Here we examine what effect this might have had on the published color excess for the star.

The magnitude difference in Aitkin is given as 0.2 mag, with no spectral type given for star B. Without a spectral type or any other means of estimating the intrinsic $B-V$ color of the companion, we cannot make a definitive estimate of its contribution to the color excess of the system. We can only carry out an example calculation, to illustrate the possible effect. If we make the conservative assumption that the secondary is a late-type star (say an M star) having $(B-V)_o = +1.2$, along with the assumption that the primary (a B5 V star) has $(B-V)_o = -0.20$, and we constrain the system to have composite magnitudes $V = 8.53$ and $B = 9.21$ with the visual magnitude difference between the two stars being $m_{A-B} = -0.20$, we find the intrinsic color of the system to be $(B-V)_{A+B} = 0.23$, yielding a color excess $E(B-V) = 0.45$.

It is, in fact, unlikely that the companion is a late-type star, for two reasons: (1) if it were a cool star but only 0.2 mag fainter in V than the primary, then the spectrum should be composite, showing some features due to the cool star, and nothing of the sort is reported in the literature (and nothing resembling a cool-star spectrum appears in our data); and (2) any cool companion that was comparable in brightness to the primary would have to be an evolved star of lower mass, and this could not have happened unless the system were of the Algol type. But it is not a close binary, since it is visual, so the mass transfer required for the Algol phenomenon to occur would have been very unlikely. Hence we expect that the secondary star is of early spectral type, probably a slightly later B star than the primary. In that event, there is little or no effect on the value of $E(B-V)$ as derived from standard photometry. Also low-resolution *IUE* spectra, used for determining the extinction law toward BD +31°643 in § 4, show no evidence of the secondary's spectrum.

3. CFHT OBSERVATIONS AND DATA ANALYSIS

Spectroscopic observations of BD +31°643 were obtained at the 3.6 m Canada-France-Hawaii Telescope on two occasions, in 1989 August, when data in the yellow-red portion of the spectrum were obtained, and in 1990 September, when blue-wavelength spectra were obtained. In both cases the instrument used was the coudé spectrograph with an 1872 diode Reticon detector, achieving approximately a 2 pixel resolution as measured by the calibration lamps. The red spectra were obtained in first order, which yielded a dispersion of 0.069 Å per diode, corresponding to a 2 pixel velocity resolution at the Na I D lines of about 7 km s^{-1}. The blue spectra were obtained in second order, yielding a dispersion of 0.035 Å per diode and a 2 pixel velocity resolution at 4000 Å of about 5 km s^{-1}. The resulting wavelength coverage was

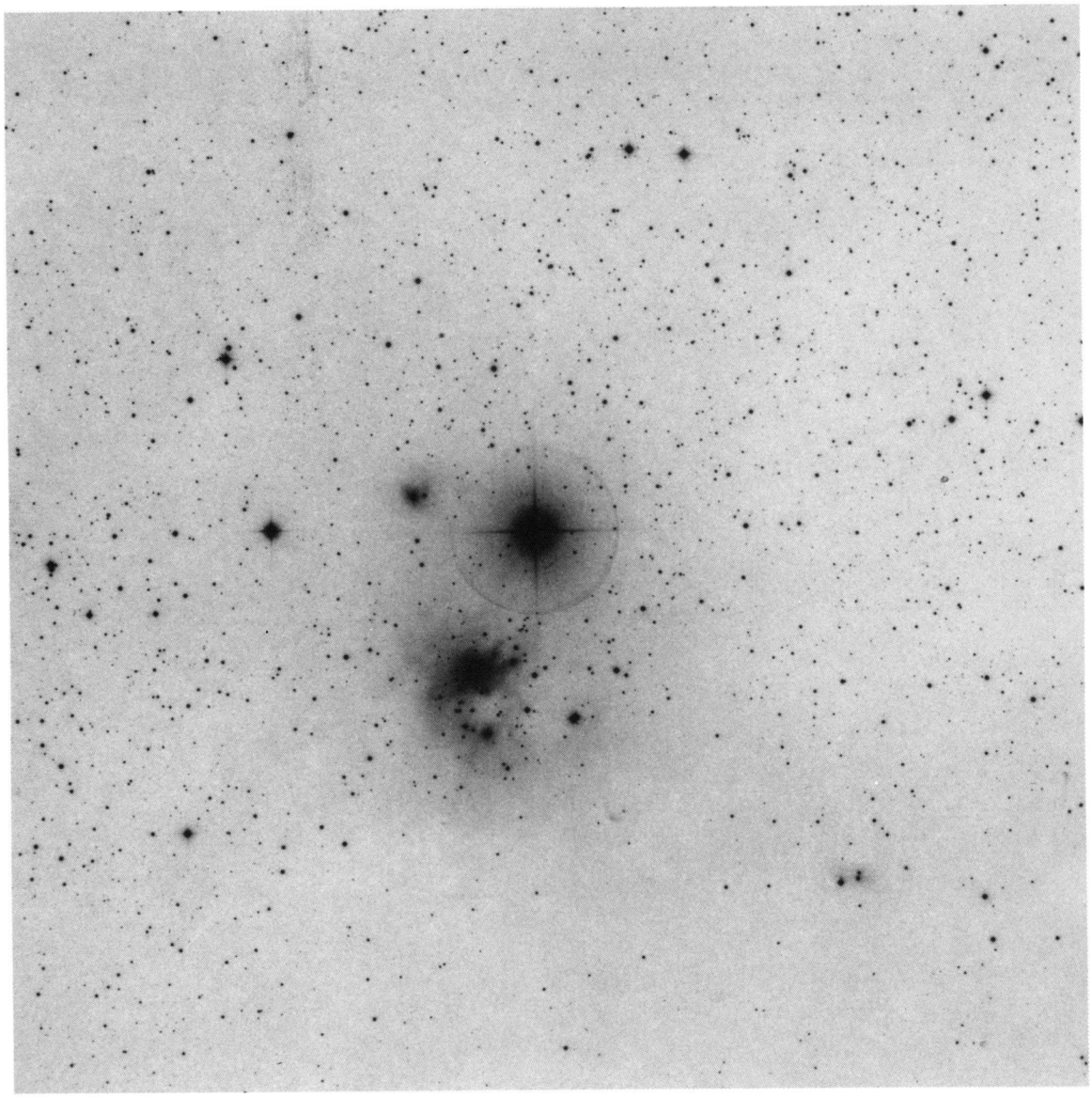

FIG. 1*a*

FIG. 1.—Reproductions from the Palomar Plate Survey in the region of IC 348. Fig. 1*a* is the red plate, 1*b* is the blue. *o* Per is the very bright star at the center. BD +31°643 is within the dark nebular region to the south–southeast of *o* Per.

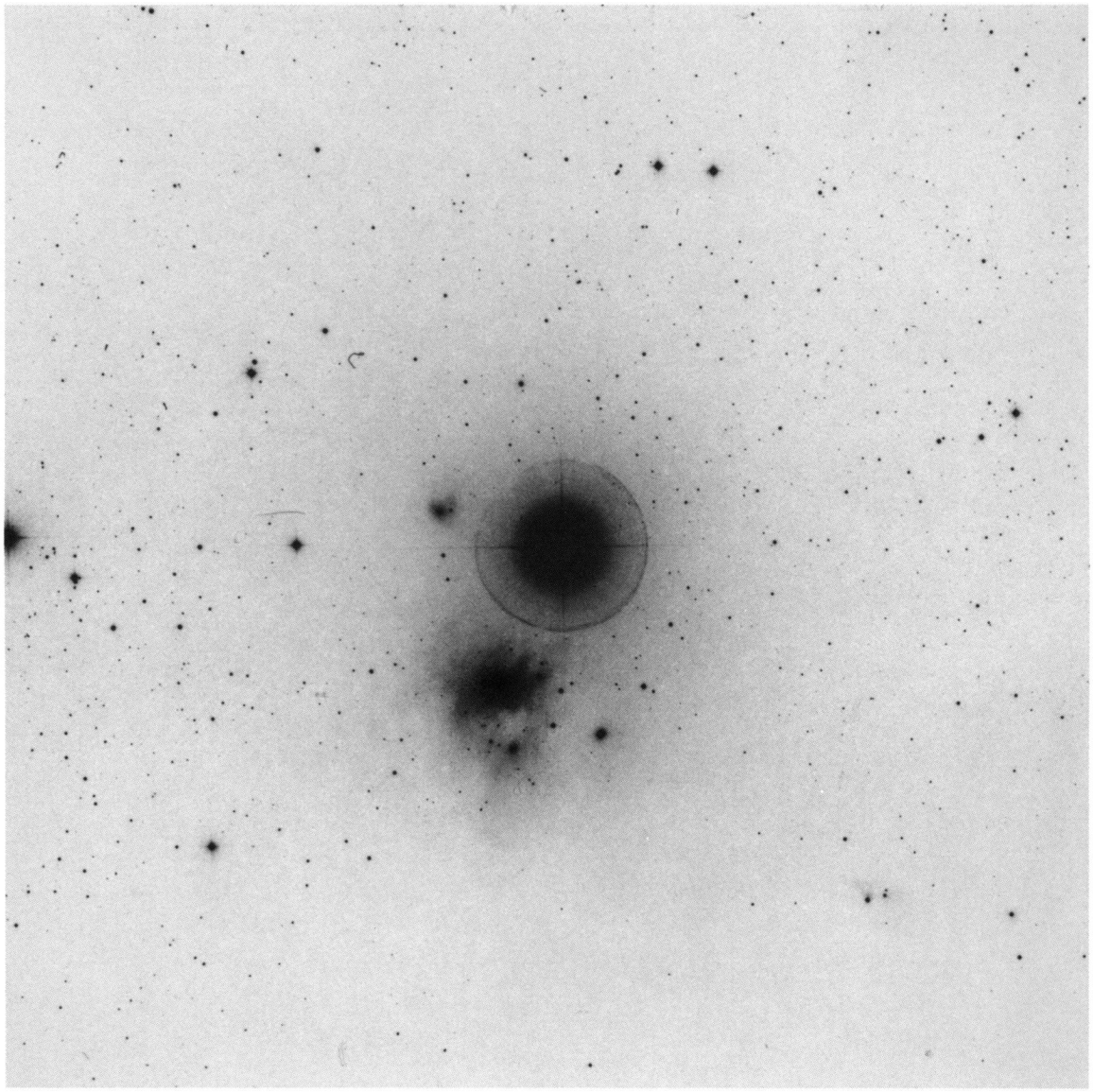

FIG. 1*b*

SNOW et al. (see 420, 633)

roughly 65 Å per exposure in the blue, and about 130 Å in the red.

Data reduction for the Reticon spectra is quite straightforward, with much of the instrumental signature (such as a four-channel fixed-pattern ripple that is introduced by the electronics) removed automatically at the telescope. Calibration Ne-Th lamp spectra were obtained before and after each grating setting, and quartz-halogen lamp spectra were obtained for each wavelength setting as well, for use in removing flat-field structure due to variations in gain from diode to diode. The flat-field exposures were long enough to ensure that the photon noise was smaller than the noise in the stellar spectra. Division of the flat-field spectra and calibration of the wavelengths (including reduction to heliocentric wavelength scales) were accomplished at the University of Colorado. Absolute calibration of the spectrum containing the 4232 Å CH^+ line was not possible, due to irreparable calibration errors in that order; however, the equivalent width is accurate. Fortunately the velocity of the 3957 Å CH^+ line can be measured quite accurately, because it lies between the two Ca II lines.

The resulting signal-to-noise ratios for the BD +31°643 spectra ranged from 20 (for the shortest blue wavelength observed) to about 260 (at the D lines), where the quantum efficiency of the Reticon is better. The 1 σ equivalent width uncertainties listed in Table 1 were computed following the convention of Jenkins, Jura, & Loewenstein (1983). Example spectra are shown in Figure 2.

Equivalent widths (or upper limits) are presented in Table 1, along with the oscillator strengths for the observed transitions. Column densities were derived following standard curve-of-growth methodology, with the usual uncertainties, dominated by the difficulty in establishing the velocity dispersion parameter b. In this case these uncertainties were reduced substantially, at least for the species expected to arise in the cold, dense cloud core, because we were able to estimate b by two methods, which agreed well with each other. First, the curve-of-growth fitting itself can yield the b-value, if multiple lines of a given species are observed, and if these lines fit a single b-value. Included in our data were three pairs of lines from common species: Na I, Ca II, and CH^+. The Na I lines fitted the curve for $b = 1.5$ km s^{-1}, as did the CH^+ lines (Fig. 3), whereas the Ca II lines indicated a value of $b = 4.0$ km s^{-1}. The two distinct b-values probably indicate differences in the spatial extent of the species; we were surprised to find that CH^+ fitted the same curve as Na I (this is discussed later).

The second method for establishing the velocity dispersion parameter was to use the measured velocity widths of radio emission lines that appear to arise from the same gas as the optical absorption lines. As already noted, we believe this to be the case for several species, including CO, OH, and CH. The line widths (FWHM) for these radio emission lines all lie within a narrow range, between 2.3 and 3.0 km s^{-1} (Sancisi et al. 1974; Zuckerman & Turner 1975; Lang & Willson 1978), corresponding to b-values in the range 1.4–1.8 km s^{-1}. Thus it appears reasonably well established that a b-value of 1.5 km s^{-1} is a good representation of the cold, dense gas in the line of sight. Thus the column densities of all species except Ca II were derived assuming $b = 1.5$ km s^{-1}. For Ca II, the two observed lines do not conform to the same velocity dispersion parameter, probably because Ca II arises along an extended path length beyond the confines of the cold, dense region where the neutral atoms and molecular species exist. Column densities are listed in Table 1.

4. THE ULTRAVIOLET EXTINCTION CURVE

Low-dispersion *IUE* spectra of BD +31°643 were obtained in 1980, as part of the doctoral dissertation research by one of us (C.G.S.; Seab 1982) and the extinction curve was originally published by Seab & Snow (1984). In the present study, the curve has been reextracted using superior routines and rederived, using standardized techniques that allows more rigorous comparison with results for other clouds.

The *IUE* data were extracted using the weighted slit extraction routine OPTIMAL (Kinney, Bohlin, & Neill 1991) available at the University of Colorado Regional Data Analysis Facility (CURDAF). A higher signal-to-noise spectrum is obtained by use of a more sophisticated fit to the cross-dispersion profile, while still preserving total flux and removing most of the cosmic-ray spikes.

The ultraviolet extinction curve toward BD +31°643 has been determined using the "pair method" of Fitzpatrick & Massa (1986). In this method, a lightly reddened comparison star is used as a flux standard whose spectral features match

TABLE 1

CFHT OBSERVATIONS

Species	λ(Å)	f[a]	V (km s^{-1})	W_λ (mÅ)	σ (mÅ)	log N (cm^{-2})	b (km s^{-1})
Na I	5889.9512	0.6311	+8.0[b]	206	0.37	14.20	1.5
Na I	5895.9243	0.3180	+7.1[b]	225	0.37		
Al I	3961.520	0.1129	...	≤3.2	1.6	≤11.30	
Ca I	4226.728	1.753	...	≤1.8	0.9	≤9.81	
Ca II	3968.468	0.3145	+14.6	64.6	9	12.36	4
Ca II	3933.663	0.6349	+14.6	105	5		
Ti I	3962.851	0.01362	...	≤4.0	2.0	≤12.32	
Fe I	3859.9111	0.02166	...	≤5.0	2.5	≤12.24	
CH	4300.3132	0.00506	+14	30.4	0.49	13.72	1.5
CH^+	4232.548	0.00545	...	38.4	0.90	13.92	1.5
CH^+	3957.692	0.00331	+16.2	29.2	1.8		
CN	3874.607	0.034	...	≤5.0	2.5	≤12.04	

[a] Oscillator strengths for the atomic lines are from Morton 1991. Oscillator strengths for the molecular transitions are from van Dishoeck & Black 1986.

[b] The velocities for the Na I lines are very uncertain, due to the fact that they were placed near the end of the observed section of the spectrum and there were no calibration lamp lines nearby. Other velocities are certain to ±3 km s^{-1}.

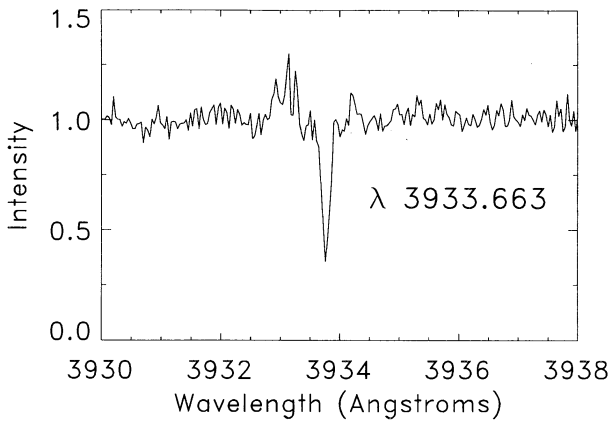

FIG. 2a

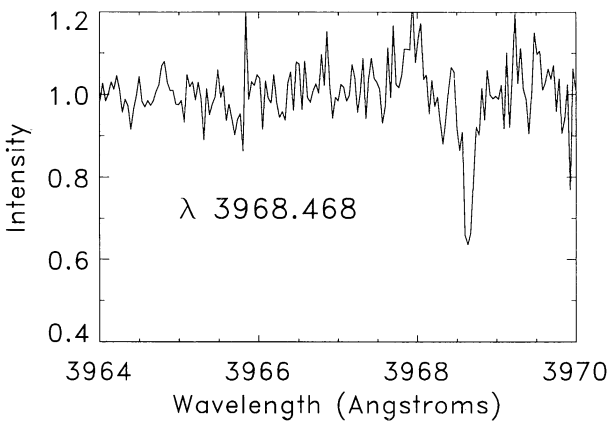

FIG. 2b

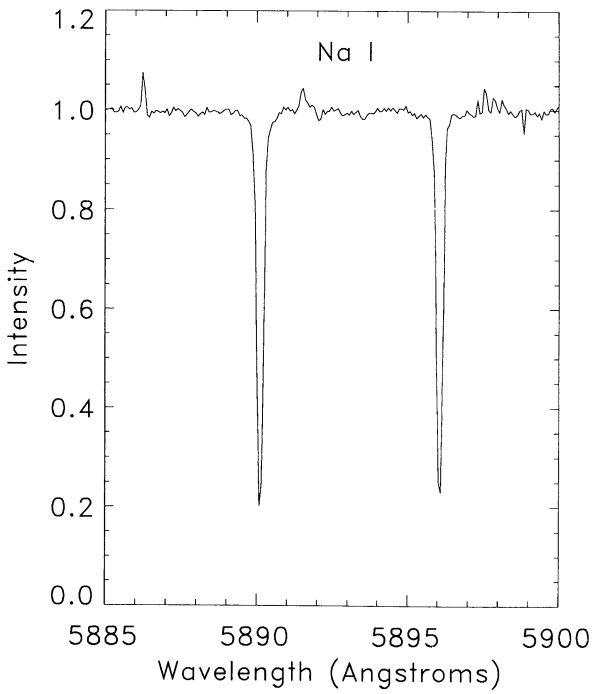

FIG. 2c

FIG. 2.—CFHT optical spectra toward BD +31°643. Figs. 2*a* and 2*b* show the Ca II lines; Fig. 2*c* shows the Na I doublet in the red. Signal-to-noise ratio is approximately 20 for the Ca II lines and about 250 for the Na D lines. Wavelengths are shown with reference to heliocentric velocities.

those of the reddened star. The comparison star's flux distribution is dereddened using the average interstellar extinction curve (Savage & Mathis 1979). Then the flux distributions of the two stars are compared and normalized to the visual color excess $E(B-V)$, with the resulting extinction curve being expressed in terms of the ratio $E(\lambda-V)/E(B-V)$.

The comparison stars used in deriving the extinction curve for BD +31°643 were HD 34759 (spectral type B5 V; color excess $E(B-V) = 0.01$) and HD 199081 (spectral type B5 V; color excess $E(B-V) = 0.01$). We have parameterized the derived curve using the fitting routine of Fitzpatrick & Massa (1990). This results in a six-parameter fit, with one parameter corresponding to the central wavelength of the 2175 Å extinction bump, another to the width of the bump, and four more that are related to the slope and the curvature of the underlying curve. In Figure 4, the extinction curve toward BD +31°643 is shown, along with the R-dependent extinction curves of Cardelli, Clayton, & Mathis (1989) (*solid line*) for $R = 3.3$ and 4.3. As a comparison, the curve for ρ Oph is also given (*dashed line*). The values for the six Fitzpatrick & Massa parameters are listed in Table 2, along with the expected values for normal R-dependent extinction (Cardelli et al. 1989).

We chose to show the fits from both comparison stars, to serve as an estimate of the possible errors associated with such determinations. The pair method is subject to both random and systematic errors, which have been outlined by Massa, Savage, & Fitzpatrick (1983). The largest source of error is through spectral mismatch. We have chosen two stars that appear to match extremely well with BD +31°643. Despite their identical spectral classification (in the optical) and visual inspection of the stellar lines in their UV spectra, they do not give identical coefficients. We have attempted to evaluate our errors by using the average of the two curves as a more reliable comparison, and noting the range over which the two standard stars differed. Fitzpatrick & Massa (1990) list 1 σ errors intrinsic to their fitting routine. For the most part, the range in extinction coefficients derived for BD +31°643 from the two standard stars seems reasonable and can mostly be attributed to intrinsic errors in the fitting routine. While we have no way of knowing without doubt that the spectral matches are good,

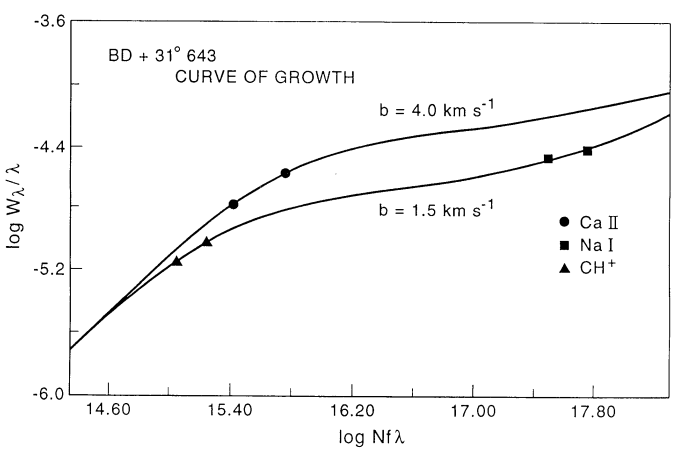

FIG. 3.—Curves of growth for the atomic species and CH^+ seen toward BD +31°643. Na I and CH^+ fit the curve with a Doppler b-value of 1.5 km s^{-1}, while Ca II fits the curve for a Doppler b-value of 4.0 km s^{-1}.

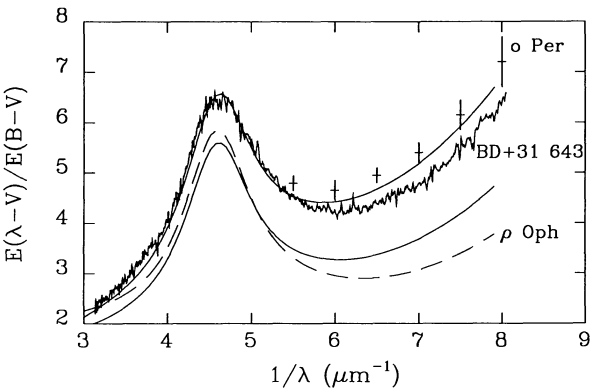

FIG. 4.—The extinction curve of BD +31°643. Also plotted as solid lines are the R-dependent extinction curves of Cardelli et al. (1989). The crosses represent the extinction law toward o Per, taken from Snow (1976). The dash curve is the extinction law toward ρ Oph taken from Fitzpatrick & Massa (1990). The upper solid curve is the R-dependent CCM curve for $R = 3.3$ while the lower solid curve is the CCM curve for $R = 4.3$.

the values from two different comparison stars are nearly consistent within the fitting errors alone.

The R-dependent extinction law of Cardelli et al. (1989) has been empirically determined, as previous laws have (Seaton 1979; Savage & Mathis 1979); however, they have "removed" an underlying variation overlooked in previous work. R, the ratio of total-to-selective extinction, and its correlation with optical polarization, has generally been understood to trace differences in grain size distributions (Serkowski, Mathewson, & Ford 1975; Clayton & Mathis 1988). We would expect a variation in average size distributions to have an effect in the UV. As in the optical, in sight lines with large R values, the extinction in the UV is grayer; i.e., less sensitive to wavelength (selective extinction) for the same total visible extinction. This has the effect of changing the underlying slope of the UV extinction curve without necessarily changing the characteristics of the bump and far-UV rise. By taking this effect into account, average extinction curves as a function of R were determined by Cardelli et al. (1989). We have given the coefficients for the Fitzpatrick & Massa parameterizations for the appropriate R-dependent curves in Table 2. Conversion from a normalization of $E(B-V)$ as we have done and was done by the series of Fitzpatrick & Massa papers to a normalization of A_V, as done with Cardelli et al. (1989), is simply $a_1 = c_1/R + 1$, $a_2 = c_2/R$, $a_3 = c_3/R$, and $a_4 = c_4/R$, where the a's are the coefficients when normalized to A_V (Cardelli & Clayton 1991).

Now that the R-dependent nature of UV extinction curves is known, other variations in UV grain properties, such as in the 2175 Å bump and in the far-UV, can be sought. A number of authors have studied the variation of UV extinction specific to environmental conditions in light of the R-dependent law (Cardelli & Clayton 1988; Cardelli & Savage 1988; Cardelli & Clayton 1991), but the most recent study by Mathis & Cardelli (1992) has shown statistically significant systematic deviations from the R-dependent law for certain environmental conditions, indicating systematic changes of grain properties in dark clouds and bright nebulae versus the general diffuse interstellar medium.

BD +31°643 has been likened to the ρ Oph cloud in its optical and near-IR extinction and bright nebular properties (Strom et al. 1974). As seen in Figure 4, the far-UV extinction rise for BD +31°643 lies slightly below the average interstellar curve, though not as far below as the notoriously shallow far-UV rise of ρ Oph and other stars in the ρ Oph cloud (Bless & Savage 1972; Snow & York 1975; Bohlin & Savage 1981; Massa et al. 1983). Comparison of the six-parameter fit with those compiled for several stars by Fitzpatrick & Massa (1986, 1988) shows that BD +31°643 has a broader bump than the average curve for the appropriate R (Cardelli et al. 1989). At the same time, the curve for BD +31°643 has a shallower slope than the average curve (indicated by parameter c_2) but a similar curvature (c_4).

This curve is quite unusual in that it shows characteristics that are normally not seen together. From the earliest observations of UV extinction curves, it has been recognized that there are very large contrasts in curve shape in different regions (e.g., Bless & Savage 1972; Massa et al. 1983; Fitzpatrick and Massa 1986, 1988, 1990). Some systematic behavior has been noted (see Fitzpatrick and Massa 1988; Snow 1992; Mathis & Cardelli 1992), such as a tendency for curves having very steep far-UV extinction rises to also have somewhat broadened 2175 Å bumps, whereas curves having shallow far-UV rises tend to have narrow bumps. These contrasts have been linked to other cloud properties, such as internal radiation field (see Mathis 1990), molecular content (e.g., Joseph et al. 1986; Cardelli 1988; Joseph, Snow, & Seab 1989; Snow 1992), depletions of elements from the gas onto the dust (Joseph et al. 1986), and even the behavior of the unidentified diffuse interstellar bands (Krelowski et al. 1993).

The extinction curve for BD +31°643, however, shows features of both types of curves. The 2175 Å bump is somewhat broader than average, a phenomenon usually associated with a steep far-UV rise; this is consistent with the curve for o Per, which has a broad bump and a steep rise (Snow 1976; Clayton & Hanson 1993). On the other hand, the far-UV rise is some-

TABLE 2

EXTINCTION CURVE DATA FOR BD +31°643

STANDARD STAR	λ_0^{-1}	γ	CURVE COEFFICIENTS c_1	c_2	c_3	c_4
HD 34759	4.603	1.128	0.3956	0.541	4.640	0.535
HD 199081	4.605	1.173	0.108	0.540	4.963	0.516
Average (range)[a]	4.604(0.002)	1.15(0.05)	0.3(0.2)	0.541(0.001)	4.8(0.3)	0.53(0.02)
CCM[b] ($R_V = 3.3$)	4.602	0.99	−0.07	0.67	3.47	0.52
Errors[c]	0.007	0.02	0.2	0.04	0.15	0.05

[a] Absolute range in coefficient value between the two standard stars.
[b] From Cardelli, Clayton, & Mathis 1989 and converted for the $E(B-V)$ normalization.
[c] Approximate error in coefficient value, from Table 7 in Fitzpatrick & Massa 1990.

what shallower than in the average curve (and shallower than in the curve for o Per).

Thus the dust toward BD +31°643 displays a mixture of properties and may well consist of distinct regions having different histories. It has been shown (Fitzpatrick & Massa 1988; Snow 1992) that the curves having narrow bumps and shallow far-UV extinction often characterize dust in young clusters and star-formation regions. In at least one well-studied case, the ρ Oph cloud, it has been suggested that grain coagulation is responsible (Jura 1980), thus altering the grain size distribution to reduce the number of small particles that are normally responsible for the far-UV extinction rise. It has also been pointed out (Snow 1983b) that coagulation reduces the grain surface area available for forming H_2, which helps to explain the low molecular fraction in such regions (but undoubtedly the high internal radiation field also contributes to the suppression of molecules).

The composite nature of the extinction curve toward BD +31°643 suggests that the line of sight contains distinct regions having different dust properties, and that these regions are competitive with each other in contributing to the overall extinction. One region, lying in front of the cluster IC 348 and in front of o Per as well, is characterized by a steep far-UV extinction rise. The other, lying within the cluster, is characterized by low far-UV extinction. The result is a curve that has only moderately shallow far-UV extinction and a broad bump that is normally associated with a steep far-UV rise (Cardelli & Savage 1988).

We can speculate that originally all the dust in the region was the same, as represented by the o Per extinction curve, but that in a dense concentration where recent star formation has occurred, the dust has been modified and now closely resembles that in the ρ Oph cloud and other young clusters.

5. *IRAS* MAPS

We have obtained *IRAS* images of the field that includes IC 348 and o Per, taking advantage of revised data processing techniques that provide improved spatial resolution over the 1′ or so that was standard in the initial data release. The new 12 and 60 μm images are shown in Figure 5, on which the positions of BD +31°643 and o Per are indicated. These plots have been made to match the scale of Figure 1 so they can be directly compared.

Both maps show a peak in far-infrared intensity centered precisely on the position of BD +31°643; the peak in the 60 μm map is unresolved and apparently symmetric, while the peak in the 12 μm map is somewhat elongated toward the southwest. Both maps also show a large-scale extension toward the southwest, extending to at least 30′ away.

No detailed spectral information in the far-infrared is available, so we cannot determine whether the 12 μm emission that is seen consists of discrete bands or continuum emission. The possibility that it is due to discrete bands is raised by the ubiquitous unidentified infrared emission features (UIRs), which have been associated with emission by polycyclic aromatic hydrocarbon molecules (PAHs; Duley & Williams 1981; Léger & Puget 1984; see the reviews published by Allamandola 1989 and by Allamandola, Tielens, & Barker 1989). There is widespread evidence that 12 μm emission observed by *IRAS* is generally due to UIR emission, particularly the strong feature at 11.3 μm (Giard et al. 1988a, b; Puget 1989). Thus it is possible that the strong peak in 12 μm emission surrounding the position of the star is due to PAH emission bands, which are normally seen in regions having a strong source of UV photons to excite the PAHs.

The 60 μm peak, however, is not due to PAH emission, since there are no known bands in this wavelength region, but instead is thought to be continuum emission due to warm dust grains. The fact that the 60 μm peak is sharper than the 12 μm peak therefore suggests that the radiation intensity needed to excite the PAH emission is less than that needed to heat the grains enough so that they emit strongly in the 60 μm band.

In order to check whether the peaks in far-IR emission represent localized heating rather than being density peaks, we constructed temperature maps using a two-component fitting procedure developed by one of us (J.M.S.) for a survey of *IRAS*

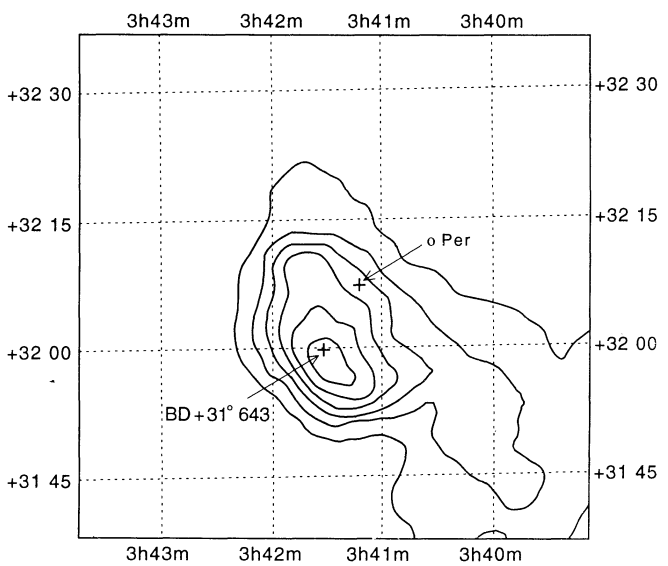

FIG. 5a

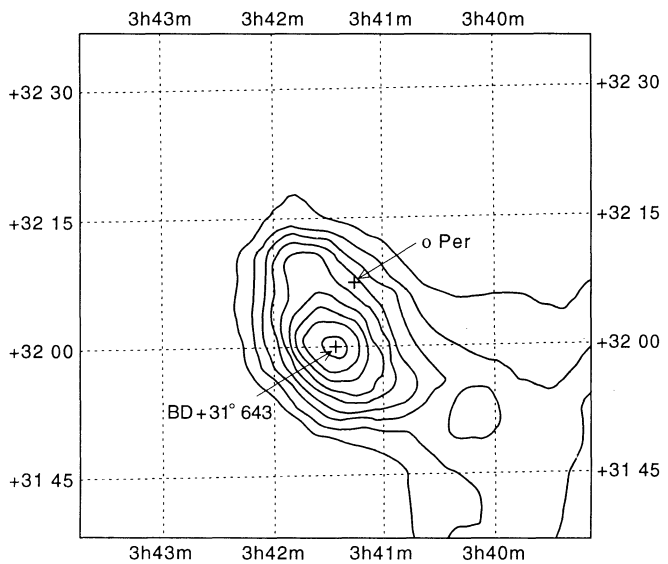

FIG. 5b

FIG. 5.—The *IRAS* 12 μm (*a*) and 60 μm (*b*) maps of IC 348. The positions of o Per and BD +31°643 are indicated. The map covers the same sky area as Figs. 1*a* and 1*b* and can be directly compared with those images.

detected supernova remnants (Saken, Fesen, & Shull 1992) using the method of Draine (1990). The grains were assumed to emit as blackbodies modified by an emissivity law, $(\lambda_0/\lambda)^{1.5}$, where $\lambda_0 \approx 0.2$ μm. Fluxes for each *IRAS* band ($i = 1, 2, 3, 4$) were calculated using the formula,

$$F_i = b_1 \int B_\lambda(T_1)(\lambda_0/\lambda)^{1.5} R_i(\lambda) d\lambda + b_2 \int B_\lambda(T_2)(\lambda_0/\lambda)^{1.5} R_i(\lambda) d\lambda \,. \quad (1)$$

Here B_λ is the Planck function, $R_i(\lambda)$ is the response function of the *IRAS* detectors, and a factor of π in the astrophysical flux has been subsumed into the constants b_i.

The fluxes F_i were then fitted to the observed fluxes on a pixel-by-pixel basis in order to determine the weighting coefficients (b_1, b_2) and the average temperatures (T_1, T_2) for components 1 and 2, respectively. The four *IRAS* fluxes exactly constrain the model.

The resulting maps are shown in Figure 6. Figure 6*a* is the "hot" component, reflecting the ensemble of small, stochastically heated grains that dominate the emission at 12 μm. Figure 6*b* is the "cold" component, reflecting the larger grains that represent almost all the dust mass and dominate the emission at 60 (typically) and 100 μm. The resolution is courser than is seen in Figure 5, because Figure 5 was produced from *IRAS* images that had been especially processed to enhance spatial resolution. Nevertheless, in Figure 6 it is clear that both populations of grains are heated in a localized region that is centered precisely on the position of BD +31°643. Within the cloud, the small ensemble of grains has an average temperature range of 168–192 K, while the larger ones have a range of 26–38 K. Thus the peaks in the *IRAS* intensity maps seen in Figure 5 are definitely due to local heating, independently of whether there may be a density enhancement in the region as well.

The *IRAS* data indicate that the observed interstellar material is intimately involved with BD +31°643, since it is clear that the star is the exciting source. This supports our discussion earlier, in which we placed the cluster IC 348 within the expanding shell of gas that lies in front of *o*, ζ, and ξ Per. The effects of the strong UV radiation field on the gas are discussed in the next section.

6. RESULTS AND DISCUSSION

6.1. *Total Gas Column Density and Molecular Fraction*

In order to compare the sight line toward BD +31°643 with those toward nearby stars such as *o* Per, and to derive depletions, it is necessary to determine the total gas column density toward BD +31°643. The star is too faint for high-dispersion ultraviolet spectroscopy (even with the *HST* the shorter wavelength regions of the spectrum require prohibitively long exposure times, at least in the high-dispersion mode); so while H I measurements may be possible using a low-dispersion mode on the *HST*, direct measurements of the Lyman and Werner bands of H_2 are not feasible at the present time.

Based on extinction and radio emission-line data, however, we can estimate the total gas column density with some reliability. This is made possible by the existence of radio and extinction data on *o* Per and the assumption, supported by the discussion in § 2, that the latter lies behind the same shell of gas in which BD +31°643 is embedded. It is also very useful to assume that the same gas is observed in radio emission as in optical/UV absorption. Strong support for this assumption comes from the good match between the observed velocities of the radio and optical/UV lines: the 21 cm H I emission, as well as the radio CH, OH, and CO emission, occur at the same velocity as the optical absorption (see Table 3).

The total gas column density may be estimated in a couple of ways: (1) by scaling relative to some observed element that is thought to be undepleted; or (2) by scaling relative to the total extinction. Sodium is usually found to be little depleted (e.g., Morton 1975), and is the only such species available to us for BD +31°643. Taking the Na I column densities for *o* Per from

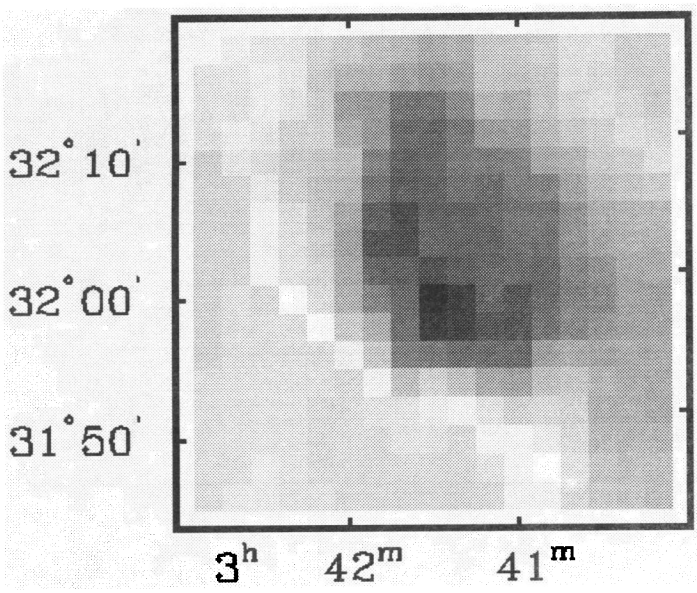

FIG. 6*a*

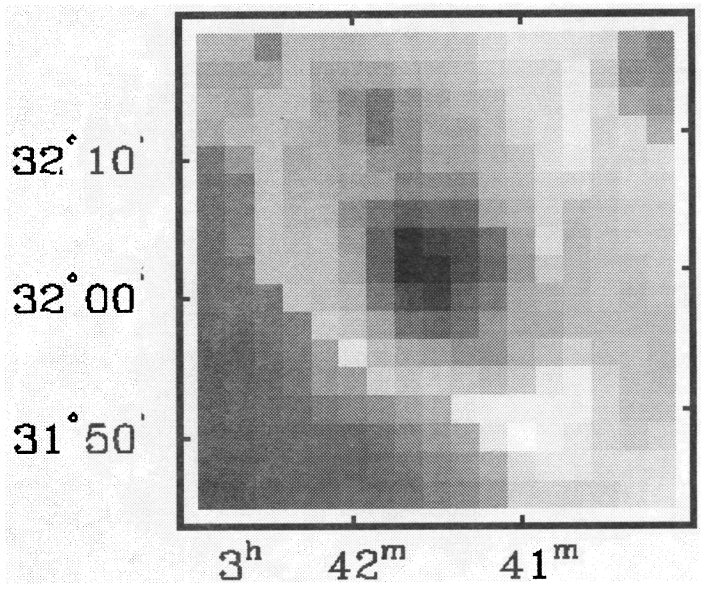

FIG. 6*b*

FIG. 6.—Modeled grain temperature maps for (*a*) the "hot" component, dominated by small stochastically heated grains, and (*b*) the "cold" component, dominated by large dust grains. See § 5 in the text for more details on the model used.

TABLE 3

SUMMARY OF LITERATURE RADIO DATA

Species	Beam Size	Transition	Frequency (MHz)	V (km s^{-1})	δV (km s^{-1})	Reference
H I	36′	$^2S_{1/2}$ $F = 0-1$	1420.405	+13	3	1
CH	9′	(1 − 1)	3335.478	+13.2	3	2, 3, 4
OH	29′		1665.40, 1667.36	+13.4	3	5
CO	1′.1	$J = 1 \rightarrow 0$	115.271(GHz)	+13.3	1.8	6
^{13}CO	1′.1	$J = 1 \rightarrow 0$	110.201(GHz)	+13.3	1.4	6
H_2CO	10′		4829.660	+14.3	1.1	7

REFERENCES.—(1) Sancisi 1974; (2) Zuckerman & Turner 1975; (3) Lang & Willson 1978; (4) Willson 1981; (5) Sancisi et al. 1974; (6) Kutner et al. 1980; (7) Dieter 1973.

the compilation of Snow (1976) and for BD +31°643 from this study (§ 3), we find from their ratio that the column density of hydrogen toward BD +31°643 is $N(\mathrm{H}) = 2.5 \times 10^{21}$ cm^{-2}. There is some uncertainty in this value because Na I is not the dominant state of ionization for sodium in H I regions, and there is evidence (discussed later) that the degree of ionization may be higher toward BD +31°643 than toward o Per. Thus the comparison of Na I column densities may underestimate the hydrogen abundance toward BD +31°643.

Use of the observed extinction value to derive the total gas column density may be accomplished using the results from Bohlin, Savage, & Drake (1978), who found from *Copernicus* data that on average diffuse clouds have a ratio $N(\mathrm{H})/E(B-V) = 5.8 \times 10^{21}$ cm^{-2} mag^{-1}. If we insert $E(B-V) = 0.84$ we find $N(\mathrm{H}) = 4.9 \times 10^{21}$ cm^{-2} for BD +31°643. For the total hydrogen column density, we adopt the mean of the two estimates based on Na I ratios and on extinction, which yields a value of $N(\mathrm{H}) = 3.7 \times 10^{21}$ cm^{-2}.

In order to derive the molecular hydrogen abundance in the line of sight toward BD +31°643, we take advantage of the fact that both CH and OH are thought to scale with molecular hydrogen (e.g., Federman 1982; van Dishoeck & Black 1986; Mattila 1986), so both may be used as indicators of the molecular hydrogen column density toward BD +31°643. In order to avoid any regional variations in the correlations that may exist, we simply scale the H_2 column density for o Per (Snow 1976) for the relative CH and OH abundances toward the two stars, arriving at $N(H_2) = 6.3 \times 10^{20}$ cm^{-2} from the CH optical data (Chaffee 1974 for o Per and this study for BD +31°643; see later sections) and 4.7×10^{20} cm^{-2} from the OH radio data (Sancisi et al. 1974). We adopt $N(H_2) = 5.5 \times 10^{20}$ cm^{-2}.

To summarize, we find the following values for the total gas column density toward BD +31°643: $N(\mathrm{H\ I}) = 2.6 \times 10^{21}$ cm^{-2}; $N(H_2) = 5.5 \times 10^{20}$ cm^{-2}; $N(\mathrm{H}) = 3.7 \times 10^{21}$ cm^{-2}. These figures are used in later sections, when we discuss depletions.

Adopting these values leads to an estimated fraction of hydrogen nuclei in the form of molecules of $f = 0.30$. This is considerably smaller than the value of $f = 0.53$ for o Per (Snow 1976), but is somewhat greater than that for the ρ Ophiuchi cloud (Snow 1983b), which may bear a strong resemblance to the IC 348 region (Strom et al. 1974). It should be emphasized here that the value of f we have derived is especially uncertain, since it comes from the ratio of two values (the column densities for atomic and molecular hydrogen) which are themselves uncertain. It is probably safest to say only that the molecular fraction in the sight line to BD +31°643 appears to be considerably lower than that for o Per (see Table 4).

6.2. *Line Velocities and the Spatial Distribution of the Gas*

The radio emission data for the region of o Per and IC 348 show that both positions are covered by the same sheet of material, having an LSR velocity of approximately +7–+9 km s^{-1}, which corresponds to a heliocentric velocity for the position of BD +31°643 of +12–+14 km s^{-1}. This includes data for H I 21 cm (Sancisi 1974); OH and CH (Sancisi et al. 1974); CO (Zuckerman & Turner 1975; Kutner et al. 1980); and H_2CO (Dieter 1973). As seen in Table 2, most of the optical lines observed with the CFHT lie at the same velocity, to within the uncertainty of the measurements. Thus we conclude that the gas we are observing in the optical spectrum of BD +31°643 is physically associated with the gas that is observed in radio emission (this has already been implicitly assumed, in our discussion of velocity dispersion in the gas, in § 3).

The velocity data also support our supposition that the gas associated with IC 348 is part of the same complex of material that extends in front of o Per and other members of the Perseus II association, as pointed out by Sancisi (1974) and Sancisi et al. (1974). This makes all the more interesting the contrasts in dust properties and depletions that we find between o Per and BD +31°643, because it indicates that the differences between the two lines of sight must have arisen from local processing, not from different origins.

6.3. *Atomic Depletions*

The column densities given in Table 1 for Na I and Ca II, along with limits on a few other species, such as Ca I, Fe I, Al I, and Ti I, can be used to derive some information on depletions. The Na I data have been used to help estimate the total gas column density, as described previously. Without information on Na II, however, it is impossible to determine the total

TABLE 4

COMPARISON OF o PER AND BD +31°643

Column Density (cm^{-2}) or Parameter	o Per	BD +31°643
A_V	0.96	2.78
$E(B-V)$	0.32	0.84
$N(\mathrm{H\ I})$	7.4×10^{20}	(2.6×10^{21})
$N(H_2)$	4.1×10^{20}	(5.5×10^{20})
N_{H}	1.6×10^{21}	(3.7×10^{21})
$f = \frac{2N(H_2)}{N(\mathrm{H\ I}) + 2N(H_2)}$	0.52	(0.30)
$N(\mathrm{CN})$	3.3×10^{12}	$\leq 1.1 \times 10^{12}$
$N(\mathrm{CH})$	3.4×10^{13}	5.3×10^{13}
$N(\mathrm{OH})$	1.3×10^{14}	1.5×10^{14}
$N(\mathrm{CH}^+)$	4.8×10^{12}	8.3×10^{13}
Ca Depletion (dex)	−3.02	−3.55

sodium column density, nor to determine the ionization balance within the observed gas. There are indications that the gas close to BD +31°643 may be more highly ionized than in the rest of IC 348, in that the radio CO data show enhanced collisional excitation in the region and a "hole" in the overall CO abundance centered on the star's position (Kutner et al. 1980). This kind of situation is interpreted by Kutner et al. as indicating that the local radiation field, presumably in this case from BD +31°643 itself, is inhibiting molecular formation (via photodissociation) despite the relatively high density in the gas. Further support for enhanced local radiation comes from Bachiller et al. (1987), also based on ^{12}CO and ^{13}CO maps. They find only modest radiation field enhancement near *o* Per, but greater enhancement near BD +31°643, which lies at the edge of the molecular cloud associated with IC 348. Another indication of locally intense UV radiation comes from the scattered-light analysis of Witt & Schild (1986), who find blue nebulosity to be concentrated near the star. Furthermore, as discussed in § 5, there is an infrared hot spot seen in the *IRAS* maps, centered on the star. If the radiation field is enhanced, then we would expect the ionization in the observed gas column to be enhanced as well. This is why we considered the total hydrogen column density estimate that was based on the Na I abundance to be an underestimate.

The Ca II situation is perhaps a bit cleaner, since most calcium will be in the form of Ca II (detailed calculations of ionization balance show that Ca I is negligible, and that in H I regions Ca III is normally very much less abundant that Ca II, even though Ca II ionizes to Ca III at 11.87 eV; e.g., Morton 1975; Snow 1983a).

Combining our derived Ca II column density with the estimated total gas column density yields an estimated depletion of calcium toward BD +31°643 of −3.55, assuming a cosmic calcium abundance relative to hydrogen of −5.66 (Morton 1991). For *o* Per the calcium depletion is −3.02 (Snow 1976), suggesting that depletions are enhanced in IC 348 relative to the surrounding gas. We note, however, that this suggestion is based entirely on the adopted *b*-value of 4.0 km s^{-1} for the Ca II lines. If this is in error, and a smaller *b*-value would be more appropriate, this would raise the Ca II column density and decrease the depletion.

We can obtain additional information about depletions from the relative abundances of neutral atomic species. The technique of deriving *relative* depletions based on neutral atomic column densities was explored by Snow (1984), who compared depletions found in this way with those derived directly from data on the more abundant first ions. Presumably the relative depletions based on atomic lines represent the cloud core region, whereas those based on the ions represent the integrated line of sight. In the present case, we can compare the neutral atomic column densities of Ca I, Fe I, Al I, and Ti I with that of Na I, which we take as a little-depleted standard. Doing this yields lower limits on the depletions, because we have only upper limits on the column densities.

In order to use the neutral species to estimate relative depletions in the cloud core region, it is necessary to take into account ionization equilibrium, since even in the denser portions of a diffuse cloud, the first ions will dominate (Snow 1983a). This introduces uncertainties, since the radiation field and the electron density are unknown, but fortunately these uncertainties tend to cancel out when the ratio of atomic column densities is considered (see discussion in Snow 1984).

For BD +31°643, our ratio of Ca I/Na I, combined with the ionization equilibrium considerations just described, yields a minimum depletion, relative to sodium, of −3.28 (logarithmic). Using the Ca I and Na I column densities from the literature for *o* Per, we find for that line of sight a depletion of calcium relative to sodium of −3.21. Hence the upper limit on Ca I toward BD +31°643 shows that in the cloud core calcium is at least 0.07 more depleted than in the core of the *o* Per cloud. While this difference is not significant, it is at least consistent with the indication from the Ca II results that the depletions may be enhanced in the gas associated with IC 348.

The other neutral species are not as definitive as this. The Fe I limit for BD +31°643, for example, implies an iron depletion in the cloud core that is slightly less than the depletion in the *o* Per cloud core implied by the ratio of Fe I/Na I toward that star. For Al I and Ti I, the limits are even less significant (and no data were available for these species toward *o* Per, so no comparison was possible).

Clearly it would be of interest to improve the measurements of Ca I and Fe I toward BD +31°643, since both of the current limits on these are at levels of interest for establishing the depletions in the cloud core.

6.4. *Molecular Abundances*

Our CFHT data included clear detections of CH and CH$^+$ (two lines), but only an upper limit on CN (Table 1). As already noted, the ratio of the two CH$^+$ lines fit very well to the curve of growth for $b = 1.5$ km s^{-1}, which is also the value implied by the observed widths of the radio emission lines of CO, CH, and OH. In view of the velocity shift between the radio molecular lines and the CH$^+$ lines in our data, the agreement in velocity dispersion must be viewed as a coincidence.

The ratio of CH toward BD +31°643 to that toward *o* Per is about 1.5 (this number was used in a previous section to estimate the molecular hydrogen column density, relative to that toward *o* Per). This seems consistent with the relatively higher density toward BD +31°643 (Kutner et al. 1980), and with the radio emission-line data on OH and H I, as well as the extinction map of the region (McCuskey 1938). The resulting value for the ratio of CH to total hydrogen is of order 10^{-8} and is consistent with current gas-phase chemistry models for diffuse clouds (e.g., van Dishoeck & Black 1986); although the relevence of this match is unclear in this case because there may be an extended region of atomic gas that does not contribute to the CH column density. This ratio is, however, quite different from the value found in the ρ Oph cloud stars, which typically have a full order of magnitude less CH per hydrogen nucleus (data are compiled by Cardelli & Wallerstein 1986). Thus we find that IC 348 does not appear to behave like the ρ Oph cloud in this respect.

The CN abundance toward BD +31°643 is also anomalous relative to the ρ Oph cloud. The upper limit corresponds to a ratio of CN to hydrogen of less than 3×10^{-10}, whereas for *o* Per the ratio is 2.1×10^{-9}. The column density of CN for BD +31°643 is lower than that toward *o* Per by at least a factor of 3, whereas other molecular column densities (e.g., CH and OH) are higher. In the ρ Oph cloud, CN is not detected for the brighter stars at levels corresponding to a few times 10^{-11} (Federman, Danks, & Lambert 1984), but is strong in the spectra of the most heavily reddened stars (Cardelli & Wallerstein 1986). Thus the limit for BD +31°643 is more consistent with the stars in the outer portion of the ρ Oph cloud than with the more heavily reddened stars there. This may suggest that the foreground density in front of BD +31°643 is lower

than that in the sight lines to the heavily reddened ρ Oph cloud stars, since CN is expected to be very density-sensitive (Federman et al. 1984).

This interpretation is called into question by the extinction map, as well as the radio molecular emission-line data, which show that the particle density in the IC 348 gas is high (e.g., Kutner et al. 1980). Since we already have evidence for a high radiation field intensity in the vicinity of BD +31°643, as indicated by the *IRAS* maps and the CO hole near the star (Kutner et al. 1980), and as would be expected due to the low far-UV extinction, it seems very likely that photodissociation due to a high local UV radiation field is the explanation for the low CN abundance. This would require that the observed CH arise in a lower density region elsewhere, however, since CH is also sensitive to radiation.

Perhaps the biggest surprise in the observed molecular abundances toward BD +31°643 is the large quantity of CH^+. The column density is nearly 10^{14} cm^{-1}, a factor of approximately 20 greater than that toward o Per (see Table 4), substantially larger than the column densities for the ρ Oph cloud stars (Federman 1982; Cardelli & Wallerstein 1986). The formation of CH^+ has been a problem for interstellar chemistry theory for some time, since the most probable reaction for its formation is endothermic. This led to the suggestion that it is formed in shocks (Elitzur & Watson 1978), but some of the predictions of this theory have not been borne out. For example, velocity separations between lines of CH^+ and other species should appear, but often do not; and the column density of CH^+ should not correlate with $E(B-V)$, but it does, at least crudely (Allen & Snow 1992; Gredel, van Dishoeck, & Black 1993; Allen 1994). Furthermore, if CH^+ were formed in a shock, there should be a velocity separation between CH^+ and CH, and it might be expected that the velocity dispersion for CH^+ would be larger than for the species (neutral atoms and other molecules) thought to form in cooler, more quiescent gas. But in the case of BD +31°643 this is not the case. Recall that the CH^+ lines fit the same b-value as the Na I lines, which is also the value implied by the line widths of the radio molecular emission features. The small velocity difference between CH and the 3957 Å CH^+ line does not provide evidence for a kinetic formation mechanism for the strong CH^+. The possibility that the high CH^+ abundance toward BD +31°643 is due to a radiative process is discussed elsewhere (Snow 1993).

6.5. *Diffuse Interstellar Bands*

Our CFHT data include spectra of the diffuse bands at 5780 Å and 5797 Å (Fig. 7). The equivalent widths are 299 and 89 mÅ, respectively. As seen in Figure 7, the 5780 Å band is considerably stronger and deeper than the 5797 Å feature. It was found by previous workers (Krelowski & Walker 1987; Josafatsson & Snow 1987) that these two bands do not correlate well with each other, and consequently they were assigned to distinct "families" of diffuse bands. More recently, Krelowski et al. (1993) have shown that the ratio of these two bands varies systematically with the nature of the UV extinction curve. Stars having a narrow bump and a shallow far-UV extinction rise usually have a stronger 5780 Å band, while those having a broad bump and a steep far-UV rise normally have a deeper 5797 Å band. Thus the behavior of these two diffuse bands in the line of sight toward BD +31°643 is more consistent with the former type of cloud than with the latter. Since it is not known whether the diffuse bands are formed by dust particles or molecules, it is not clear what this means.

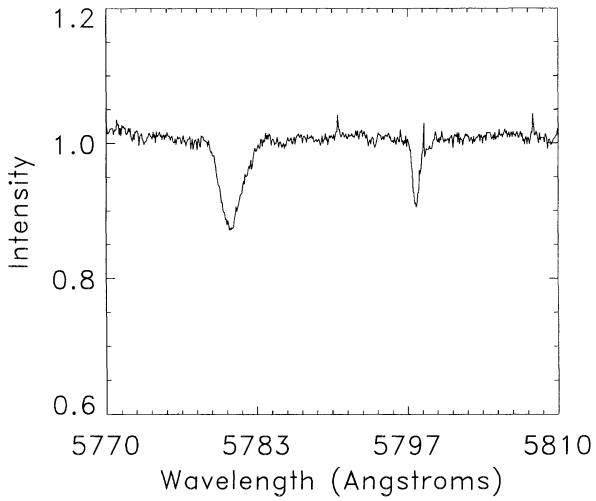

FIG. 7.—The diffuse band profiles toward BD +31°643 obtained at the CFHT.

In view of our hypothesis that the line of sight toward BD +31°643 is a composite of two distinct types of cloud material, the diffuse band results would suggest that the bands are formed predominantly within the gas and dust associated with the cluster IC 348, rather than in the foreground material. This is perhaps a bit surprising, since it has long been known that the diffuse bands are generally weak (relative to extinction) in clusters and dense cloud regions (e.g., Wampler 1966; Snow and Cohen 1974). Thus we might have expected the foreground gas and dust to dominate the diffuse band formation.

7. SUMMARY AND COMMENTS ON FUTURE WORK

Taken as a whole, the results of the present study support the view that the interstellar material within the cluster IC 348 represents a localized concentration within the widespread sheet of expanding material that lies in front of the prominent members of the Perseus II OB association. The agreement in velocity of the observed optical lines with the velocities of the radio emission features, along with the similarity of the atomic and molecular column densities, and especially the morphology of the extinction map of the region, all argue for this picture.

In this context, the most interesting of our conclusions are those showing distinct contrasts between the lines of sight to o Per and BD +31°643, which lies only about 8′ away, and is a member of a clearly delineated concentration of gas and dust within the overall distribution of otherwise homogeneous material. These contrasts include: (1) a composite UV extinction curve for BD +31°643, which appears to result from a combination of material having a broad bump and a steep far-UV rise (as in the case of o Per), and material that is characterized by a narrow bump and a low far-UV rise; (2) evidence for enhanced density and enhanced depletions within IC 348, as compared to o Per; and (3) very different molecular abundances for BD +31°643, including higher CH (and OH, as seen in the radio data), but lower CN and very much higher CH^+.

We conclude that these contrasts are the result of localized processes and conditions within IC 348, which have altered the physical and chemical state of the gas and dust. We suggest that recent star formation has caused coagulation of the interstellar dust in IC 348, which changed the grain size distribution

so that the extinction curve shows the composite properties just cited, and so that a greater concentration of UV radiation can penetrate the cloud. The enhanced density within IC 348 is the likely reason for the higher depletions relative to the *o* Per line of sight. The inferred high intensity of the radiation field near BD +31°643 is the probable cause for the diminished abundance of CN and the enhanced abundance of CH^+ (see Snow 1993). The unidentified diffuse interstellar bands at 5780 and 5797 Å show the relative strength behavior typical of other regions characterized by low far-UV extinction and recent star formation; perhaps this information will become useful as the carriers of the diffuse bands are identified.

It would be important to obtain better quality optical data on the neutral atoms and molecular species for which we currently have only upper limits and, if possible, to obtain high-resolution UV spectroscopy of other species, particularly the dominant first ions. Higher quality measurements of the velocities of the optical lines that were detected in our study would also be useful. In addition, high-quality spectra of diatomic carbon would be helpful, since C_2 has been shown to be a good indicator of both particle densities and radiation field intensities (van Dishoeck & Black 1982, 1989). This would be a very important test of our hypothesis that both the density and the radiation field intensity in the IC 348 gas are high.

This work was made possible through the allocation of observing time at the Canada-France-Hawaii Telescope, for which we are grateful, and through the award of *IUE* observations for the purpose of deriving UV extinction curves. We are indebted to the staffs of both the CFHT and the *IUE* observatories for their assistance in obtaining and analyzing the data. Much of the scientific analysis was carried out while one of us (T. P. S.) was a Visiting Research Fellow at the Research Centre for Theoretical Astrophysics, University of Sydney, an appointment which was made possible by the generous support of Professor D. B. Melrose. Data reduction at the University of Colorado was accomplished in the Regional Data Analysis Facility, supported in part by funding from the *IUE* project. Data reduction assistance was provided by K. Lawrance, R. Rudloff, and J. Boyd. Financial support has been provided by NSF grant AST-8505587 and NASA grant NSG-5300 to the University of Colorado.

REFERENCES

Allamandola, L. J. 1989, in IAU Symp. 135, Interstellar Dust, ed. L. J. Allamandola & G. G. M. Tielens (Dordrecht: Kluwer), 129
Allamandola, L. J., Tielens, A. G. G. M., & Barker, J. R. 1989, ApJS, 71, 733
Allen, M. M. 1994, ApJ, in press
Allen, M. M., & Snow, T. P. 1992, ApJ, 391, 152
Bachiller, R., Cernicharo, J., Goldsmith, P., & Omont, A. 1987, A&A, 185, 297
Blaauw, A. 1952, Bull. Astron. Inst. Netherlands, 11, 405
Bless, R. C., & Savage, B. D. 1972, ApJ, 171, 293
———. 1981, ApJ, 249, 109
Bohlin, R. C., Savage, B. D., & Drake, J. F. 1978, ApJ, 224, 132
Borgman, J., & Blaauw, A. 1963, Bull. Astron. Inst. Netherlands, 17, 358
Cardelli, J. A. 1988, ApJ, 335, 177
Cardelli, J. A., & Clayton, G. C. 1988, AJ, 95, 516
———. 1991, AJ, 101, 1021
Cardelli, J. A., Clayton, G. C., & Mathis, 1989, ApJ, 345, 245
Cardelli, J. A., & Savage, B. D. 1988, ApJ, 325, 864
Cardelli, J. A., & Wallerstein, G. 1986, ApJ, 302, 492
———. 1989, AJ, 97, 1099
Carrasco, L., Strom, S. E., & Strom, K. M. 1973, ApJ, 182, 95
Chaffee, F. 1974, ApJ, 189, 427
Clayton, G. C., & Hanson, M. M. 1993, AJ, 105, 1880
Clayton, G. C., & Mathis, J. S. 1988, ApJ, 327, 911
Crutcher, R. M. 1973, ApJ, 185, 857
Dickman, R. L. 1980, ApJ, 237, 734
Dieter, N. H. 1973, ApJ, 183, 449
Draine, B. T. 1990, in The Interstellar Medium in Galaxies, ed. H. A. Thronson & J. M. Shull (Dordrecht: Kluwer), 483
Duboshin, G. N., Dolgachev, V. P., Alinina, E. P., Rybakov, E. P., & Kholopov, P. N. 1976, Soviet Astron., 20, 392
Duley, W. W., & Williams, D. A. 1981, MNRAS, 231, 969
Elitzur, M., & Watson, W. D. 1978, ApJ, 222, L41
Federman, S. R. 1982, ApJ, 257, 125
Federman, S. R., Danks, A. C., & Lambert, D. L. 1984, ApJ, 287, 219
Fitzpatrick, E. L., & Massa, D. 1986, ApJ, 307, 286
———. 1988, ApJ, 328, 734
———. 1990, ApJS, 72, 16
Fredrick, L. W. 1956, AJ, 61, 437
Giard, M., Pajot, F., Lamarre, J. M., Serra, G., Caux, 1988a, A&A, in print
Giard, M., Pajot, F., Lamarre, J. M., Serra, G., Caux, E., Gispert, R., Léger, A., & Rouan, D. 1988b, A&A, 201, L1
Gingerich, C. H. 1922, ApJ, 56, 139
Gredel, R., van Dishoeck, E. F., & Black, J. H. 1991, A&A, 251, 625
Harris, D. L., Morgan, W. W., & Roman, N. G. 1954, ApJ, 119, 622
Herbig, G. H. 1954, PASP, 66, 19
Jenkins, E. B., Jura, M. & Loewenstein, M. 1983, ApJ, 270, 88
Johnson, H. L. 1966, ARA&A, 4, 193
Josafatsson, K., & Snow, T. P. 1987, ApJ, 319, 436
Joseph, C. L., Snow, T. P., & Seab, C. G. 1989, ApJ, 340, 314
Joseph, C. L., Snow, T. P., Seab, C. G., & Crutcher, R. M. 1986, ApJ, 309, 771
Jura, M. 1980, ApJ, 235, 63
Kinney, A. L., Bohlin, R. C., & Neill, J. D. 1991, PASP, 103, 694
Krelowski, J., Snow, T. P., Seab, C. G., & Papaj, J. 1993, MNRAS, in press
Krelowski, J., & Walker, G. A. H. 1987, ApJ, 312, 860
Kutner, M. L., Machnik, D. E., Tucker, K. D., & Dickman, R. L. 1980, ApJ, 237, 734
Lang, K. R., & Willson, R. F. 1978, ApJ, 224, L125
Léger, A., & Puget, J. L. 1984, A&A, 137, L5
Loren, R. B. 1976, ApJ, 209, 466
Lynds, B. T. 1969, PASP, 81, 496
Massa, D., Savage, B. D., & Fitzpatrick, E. L. 1983, ApJ, 266, 662
Mattila, K. 1986, A&A, 160, 157
Mathis, J. S. 1990, ARA&A, 28, 37
Mathis, J. S., & Cardelli, J. A. 1992, ApJ, 398, 610
McCuskey, S. W. 1938, ApJ, 88, 209
Morton, D. C. 1975, ApJ, 197, 85
———. 1991, ApJS, 77, 119
Papaj, J., Wegner, W., & Krelowski, J. 1991, MNRAS, 252, 403
Puget, J. 1989, in IAU Symp. 135, Interstellar Dust, ed. L. J. Allamandola & G. G. M. Tielens (Dordrecht: Kluwer), 119
Racine, R. 1968, AJ, 73, 233
Saken, J. M., Fesen, R. A., & Shull, J. M. 1992, ApJS, 81, 715
Sancisi, R. 1974, in IAU Symp. 60, Galactic Radio Astronomy, ed. F. J. Kerr & S. C. Simonson (Boston: Reidel), 115
Sancisi, R., Goss, W. M., Anderson, C., Johansson, L. E. B., & Winnberg, A. 1974, A&A, 35, 445
Sargent, A. I. 1979, ApJ, 233, 163
Savage, B. D., & Mathis, J. S. 1979, ARA&A, 17, 73
Seab, C. G. 1982, Ph.D. thesis, University of Colorado
Seab, C. G., & Snow, T. P. 1984, ApJ, 277, 200
Seaton, M. J. 1979, MNRAS, 187, 73
Serkowski, K., Mathewson, D. S., & Ford, V. L. 1975, ApJ, 196, 261
Snow, T. P. 1975, ApJ, 201, L21
———. 1976, ApJ, 204, 759
———. 1983a, ApJ, 266, 576
———. 1983b, ApJ, 269, L57
———. 1984, ApJ, 287, 238
———. 1992, Australian J. Phys., 45, 543
———. 1993, ApJ, 402, L73
Snow, T. P., Allen, M. M., & Polidan, R. S. 1990, ApJ, 359, L23
Snow, T. P., & Cohen, J. G. 1974, ApJ, 194, 313
Snow, T. P., & Jenkins, E. B. 1980, ApJ, 241, 161
Snow, T. P., & York, D. G. 1975, Ap. Space Sci., 34, 19
Strom, S. E., Strom, K. M., & Carrasco, L. 1974, PASP, 86, 798
van Dishoeck, E. F. & Black, J. H. 1982, ApJ, 258, 533
———. 1986, ApJS, 62, 109
———. 1989, ApJ, 340, 273
Wampler, E. J. 1966, ApJ, 144, 921
Willson, R. F. 1981, ApJ, 247, 116
Witt, A. N., & Schild, R. E. 1986, ApJS, 62, 839
Zuckerman, B., & Turner, B. E. 1975, ApJ, 197, 123